Available online at www.sciencedirect.com
ScienceDirect
Image and Vision Computing 25 (2007) 426–435
www.elsevier.com/locate/imavis

Attribute-space connectivity and connected filters

Michael H.F. Wilkinson *

Institute for Mathematics and Computing Science, University of Groningen, P. O. Box 800, 9700 AV Groningen, The Netherlands

Received 15 August 2005; received in revised form 17 February 2006; accepted 27 April 2006

Abstract

In this paper connected operators from mathematical morphology are extended to a wider class of operators, which are based on connectivities in higher dimensional spaces, similar to scale spaces, which will be called attribute-spaces. Though some properties of connected filters are lost, granulometries can be defined under certain conditions, and pattern spectra in most cases. The advantage of this approach is that regions can be split into constituent parts before filtering more naturally than by using partitioning connectivities. Furthermore, the approach allows dealing with overlap, which is impossible in connectivity. A theoretical comparison to hyperconnectivity suggests the new concept is different. The theoretical results are illustrated by several examples. These show how attribute-space connected filters merge the ability of filtering based on *local* structure using classical, structuring-element-based filters to the *object-attribute*-based filtering of connected filters, and how this differs from similar attempts using second-generation connectivity.

Keywords: Mathematical morphology; Connectivity; Hyperconnectivity; Multi-scale analysis; Connected filters; Perceptual grouping

1. Introduction

Semantic analysis of images always involves grouping of pixels in some way. This process is often called perceptual grouping, a concept from Gestalt psychology [1], which has also been used in the field of computer vision before [2–4]. Filters based on visual cortex models, and in particular grouping of features have already been developed [5,6]. However, they are not put in a morphological framework. In this paper I will present a method to model some aspects of perceptual grouping from the perspective of mathematical morphology, starting out with the simplest form of grouping, which is connectivity [7–9]. Connectivity allows us to group pixels into connected components or flat-zones in the grey-scale case. In mathematical morphology, *connected operators* have been developed which perform filtering based on these kinds of groupings [10–13], including attribute filters, in which filtering is based on properties (or attributes) of these "perceptual groups." However, the human observer may either interpret a single connected component of a binary image as multiple visual entities, or group multiple connected components into a single visual entity. These properties have to some extent been encoded in second-generation connectivities [8,9,14–16]. These derived connectivities are usually obtained by applying some (in general increasing) operator to the image of interest and analysing the resulting connected components. To some extent this allows a merger of the filtering based on local structure using the structuring-element-based filters, and the object-attribute-based filtering of connected filters.

A problem of connected filters is that they cannot deal with overlap. Humans have no problems in dealing with overlap when perceptually grouping image regions. A simple example is shown in Fig. 1. The cross is readily grouped into two bars, with the centre pixel belonging to both groups. Ideally we would like to allow filtering based on these higher level perceptual groups, using formalisms similar to those used in connected operators. One solution to this problem is through hyperconnectivities and hypoconnectivities [9,17]. The approach presented here is different,

* Tel.: +31 50 3638140; fax: +31 50 3633800.
E-mail address: m.h.f.wilkinson@rug.nl

0262-8856/$ - see front matter © 2006 Elsevier B.V. All rights reserved.
doi:10.1016/j.imavis.2006.04.015

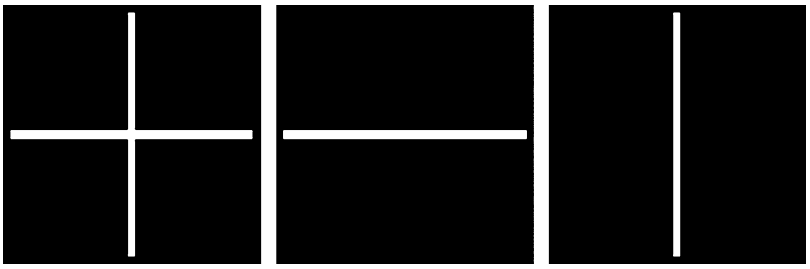

Fig. 1. Overlap in perceptual grouping: the cross (left) is perceived as two bars, one horizontal (middle) one vertical (right). The centre pixel belongs to both perceptual groups.

in that it restates the connectivity relationships in an image in terms of connectivity in higher dimensional spaces, which I will call *attribute spaces*.

In this paper I will also demonstrate a problem with partitioning connectivities when used for second-generation connected attribute filters, due to the large numbers of singletons they produce in the image. This over-partitioning effect is shown in Fig. 2. It will be shown that these attribute filters reduce to performing, e.g., an opening with ball B followed by an application of the attribute filter using the normal (four or eight) connectivity. The attribute-space approach presented here does not suffer from this, as can be seen in Fig. 2, and this leads to a more natural partitioning of the connected component into two squares and a single bridge. A similar effect is also shown in a 3D example in Fig. 9.

This paper is organized as follows. First, connected filters are described formally in Section 2, followed by second-generation connectivities in Section 3. Problems with attribute filters using partitioning connectivities are dealt with in detail in this section. Hyperconnectivities [9] are treated in Section 4. After this, attribute spaces are presented in Section 5. After some theoretical preliminaries, three examples of attribute-space connectivities are given: two based on the local width of the objects in Section 5.1 and one based on orientation in Section 5.2. In this latter section it is shown that attribute-space connectivities are not hyperconnectivities. Finally, in Section 6 a discussion of the results is given.

2. Connectivity and connected filters

As is common in mathematical morphology binary images X are subsets of some universal set E (usually $E\mathbb{Z}^n$). Let $\mathscr{P}(E)$ be the set of all subsets of E. Connectivity in E can be defined using *connectivity classes* [8,9].

Definition 1. A connectivity class $\mathscr{C} \subseteq \mathscr{P}(E)$ is a set of sets with the following three properties:

(1) $\emptyset \in \mathscr{C}$
(2) $\{x\} \in \mathscr{C}$
(3) for each family $\{C_i\} \subset \mathscr{C}$, $\cap C_i \neq \emptyset$ implies $\cup C_i \in \mathscr{C}$.

This means that both the empty set and singleton sets are connected, and any union of connected sets which have a nonempty intersection is connected.

Any image X is composed of a number of connected components or *grains* $C_i \in \mathscr{C}$, with i from some index set I. For each C_i there is no set $C \supset C_i$ such that $C \subseteq X$ and $C \in \mathscr{C}$. If a set C is a grain of X we denote this as $C \lessdot X$.

An equivalent way to view connectivity is through *connected openings*, sometimes referred to as connectivity openings [8,16].

Definition 2. The binary connected opening Γ_x of X at point $x \in E$ is given by

$$\Gamma_x(X) = \begin{cases} C_i : x \in C_i \wedge C_i \lessdot X & \text{if } x \in X \\ \emptyset & \text{otherwise.} \end{cases} \quad (1)$$

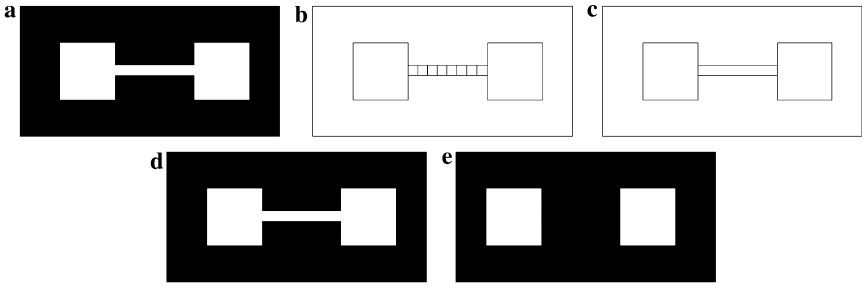

Fig. 2. Attribute-space compared to regular attribute filtering: (a) original image X; (b) the connected components of X according to $\mathscr{C}^{\psi}$, with ψ an opening by a 3×3 structuring element (see Section 3); (c) partitioning of X by attribute space method of Section 5.1; (d) regular attribute thinning $\Psi^T_{\psi}(X)$ with $T(C) = (I(C)/A^2(C) < 0.5)$; (e) attribute-space connected attribute thinning $\Psi^T_A(X)$ with the same T. T is designed to remove elongated structures. Note that only the attribute-space method removes the elongated bridge.

Thus Γ_x extracts the grain C_i to which x belongs, discarding all others.

Salembier and Serra [10] define the general class of connected filters based on partitions. A partition of E is a set of sets $\{\alpha_i\}$, with i from some index set I, such that

(1) $\cup_i \alpha_i = E$ and
(2) $\alpha_i \cap \alpha_j = \emptyset$, for all $i \neq j$.

Given two partitions $\{\alpha_i\}$ and $\{\beta_j\}$ of E, $\{\beta_j\}$ is said to be coarser than $\{\alpha_i\}$, if for any α_i there exists a β_j such that $\alpha_i \subseteq \beta_j$. Let $\mathbf{P}(X)$ denote the partition of E consisting of the connected components of binary image X and its complement.

Definition 3. A filter γ is a connected filter if, for any image X, partition $\mathbf{P}(\gamma(X))$ is coarser than partition $\mathbf{P}(X)$.

Probably the most important group of connected filters are the attribute filters, which are dealt with in the next subsection.

2.1. Attribute filters

Binary attribute openings [11,12] are based on binary connected openings and *trivial openings*. A trivial opening Γ_T uses an increasing criterion T to accept or reject connected sets. A criterion T is increasing if the fact that C satisfies T implies that D satisfies T for all $D \supseteq C$. Usually T is of the form

$$T(C) = (\mathrm{Attr}(C) \geq \lambda) \tag{2}$$

with $\mathrm{Attr}(C)$ some real-valued attribute of C, and λ the attribute threshold. A trivial opening is defined as follows $\Gamma_T : \mathscr{C} \to \mathscr{C}$ operating on $C \in \mathscr{C}$ yields C if $T(C)$ is true, and $\emptyset$ otherwise. Note that $\Gamma_T(\emptyset) = \emptyset$. *Trivial thinnings* differ from trivial openings only in that the criterion T need not be increasing. An example is the scale-invariant elongation criterion of the form 2, in which $\mathrm{Attr}(C) = I(C)/A^2(C)$, with $I(C)$ the moment of inertia of C and $A(C)$ the area [18]. The binary attribute opening is defined as follows.

Definition 4. The binary attribute opening Γ^T of set X with increasing criterion T is given by

$$\Gamma^T(X) = \bigcup_{x \in X} \Gamma_T(\Gamma_x(X)) \tag{3}$$

The attribute opening is equivalent to performing a trivial opening on all grains in the image. Note that if the attribute T is not increasing, we have an attribute thinning rather than an attribute opening [11,12]. The grey-scale case can be derived through threshold decomposition [19]. An example in the binary case is shown in Fig. 3.

3. Second-generation connectivities

Second-generation connectivities are usually defined using an operator ψ which modifies X, and a base connectivity class $\mathscr{C}$ (four or eight connectivity)[8,9,16]. The resulting connectivity class is referred to as $\mathscr{C}^\psi$. If ψ is extensive $\mathscr{C}^\psi$ is said to be *clustering*, if ψ is anti-extensive $\mathscr{C}^\psi$ is *partitioning*. In the general case, for any $x \in E$ three cases must be considered: (i) $x \in X \cap \psi(X)$, (ii) $x \in X \backslash \psi(X)$, and (iii) $x \notin X$. In the first case, the grain to which x belongs in $\psi(X)$ is computed according to $\mathscr{C}$, after which the intersection with X is taken to ensure that all grains $C_i \subseteq X$. In the second case, x is considered to be a singleton grain. In the third case the connected opening returns $\emptyset$ as before.

Definition 5. The connected opening Γ_x^ψ for a second-generation connectivity based on ψ of image X is

$$\Gamma_x^\psi(X) = \begin{cases} \Gamma_x(\psi(X)) \cap X & \text{if } x \in X \cap \psi(X) \\ \{x\} & \text{if } x \in X \setminus \psi(X) \\ \emptyset & \text{otherwise,} \end{cases} \tag{4}$$

in which Γ_x is the connected opening based on $\mathscr{C}$.

If $X \subset \psi(X)$ the second case of (4) never occurs. Conversely, if $\psi(X) \subset X$ we have $\psi(X) \cap X = \psi(X)$, simplifying the first condition in (4). In the clustering case, ψ may be a structural closing or dilation, in the partitioning case ψ may be a structural opening, but not an erosion, because the resulting connected opening would not be idempotent. An extensive discussion is given in [8,9,16].

3.1. Attribute operators

Attribute operators can readily be defined for second-generation connectivities by replacing the standard connected opening Γ_x by Γ_x^ψ in Definition 4.

Fig. 3. Binary attribute filters applied to an image of bacteria: (left) original; (middle) area opening using area threshold $\lambda = 150$; (right) elongation thinning using attribute $I/A^2 > 0.5$.

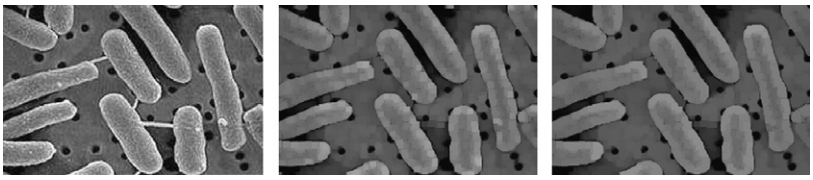

Fig. 4. Scanning electron micro-graphs of *Escherichia coli* (left to right): original image f; modified image by anti-extensive operator $\psi(f) = f \circ B_2$ with B_2 a disc with radius 2; second-generation connected area opening $\gamma_\psi^T(f)$ with $T = A(C) \geqslant \lambda$; ($\lambda = 100$). This is identical to a regular area opening $\gamma^T(\psi(f))$ with the same T. Image size 242×158 pixels.

Definition 6. The binary attribute opening Γ_ψ^T of set X with increasing criterion T, and connectivity class $\mathscr{C}^\psi$ is given by

$$\Gamma_\psi^T(X) = \bigcup_{x \in X} \Gamma_T(\Gamma_x^\psi(X)) \tag{5}$$

Though useful filters can be constructed in clustering case, and partition of grains in soil samples for computation of area pattern spectra has been used [15,20], a problem emerges in the partitioning case.

Proposition 1. *For partitioning connectivities based on ψ the attribute opening Γ_ψ^T with increasing, shift invariant criterion T is*

$$\Gamma_\psi^T(X) = \begin{cases} X & \text{if } T(\{x\}) \text{ is true for any } x \in E \\ \Gamma^T(\psi(X)) & \text{otherwise} \end{cases} \tag{6}$$

with Γ^T the underlying attribute opening from Definition 4.

Proof. If $T(\{x\})$ is true for any x, all $x \in X \backslash \psi(X)$ are preserved by Γ_ψ^T, because T is shift invariant so that $\Gamma_x^\psi(X) = \{x\}$ for those pixels. Because T is increasing and shift invariant, we have that $T(\{x\}) \Rightarrow T(C)$ for any $C \in \mathscr{C}$ with $C \neq \emptyset$. Thus, if $T(\{x\})$ is true for any x, all $x \in \psi(X)$ are also preserved, because $\Gamma_x(\psi(X)) \in \mathscr{C}$ and $\Gamma_x(\psi(X)) \neq \emptyset$ for those x. In other words if $T(\{x\})$ is true,

$$\Gamma_\psi^T(X) = X, \tag{7}$$

which proves (6) in the case that $T(\{x\})$ is true. Conversely, if $T(\{x\})$ is false for any x, all $x \in X \backslash \psi(X)$ are rejected due to shift-invariance of T, i.e., $\Gamma_T(\{x\}) = \emptyset$ for all $x \in E$. Therefore, if $T(\{x\})$ is false

$$\Gamma_\psi^T(X) = \bigcup_{x \in \psi(X)} \Gamma_T(\Gamma_x^\psi(X)). \tag{8}$$

Because all $x \in X \backslash \psi(X)$ are rejected, $\Gamma_x^\psi(X)$ can be rewritten as $\Gamma_x(\psi(X))$, and we have

$$\Gamma_\psi^T(X) = \bigcup_{x \in \psi(X)} \Gamma_T(\Gamma_x(\psi(X))) = \Gamma^T(\psi(X)). \tag{9}$$

The right-hand equality derives from Definition 4. □

Proposition 1 means that an attribute opening using a partitioning connectivity is equal to performing the standard attribute opening Γ^T on $\psi(X)$, unless the criterion has been set such that Γ^T is the identity operator. The reason for this is the fact that the grains of $X \backslash \psi(X)$ according to the original connectivity are split up into singletons by Γ_x^ψ, and these singletons are the first to be rejected as the attribute threshold is increased, for an increasing attribute such as area. This effect is shown in the grey-scale case in Fig. 4. Part (a) shows an electron micrograph of *Escherichia coli* cells interconnected by fimbriae. Part (b) shows the result of applying a partitioning connectivity operator (structural opening) on part (a). Part (c) shows the result of the second-generation connected area opening computed using the dual-input Max-tree algorithm [21] for second-generation connected attribute filters, which is identical to performing the standard area opening [22,23] on part (b) (not shown). Because of this Fig 4(a) shows clear signs of edge deformation introduced by $\psi(f)$ not characteristic of classical connected filters. Even if criteria that are not increasing are used, all structural information contained in the connected components of $X \backslash \psi(X)$ is lost, so shape information cannot be captured meaningfully by any attribute. In Section 5 a comparison with the attribute-space alternative is given and illustrated in Figs. 2 and 9.

4. Hyperconnectivities

Hyperconnectivities have been proposed by Serra [9] as a means of dealing with overlap. The idea is to relax the third constraint in Definition 1. Instead of requiring that any union of connected sets which have a non-empty intersection is connected, we use some other *overlap criterion* $\perp$ which defines when he union of hyperconnected sets is connected [17].

Definition 7. An overlap criterion in $\mathscr{P}(E)$ is a mapping $\perp: \mathscr{P}(\mathscr{P}(E)) \rightarrow \{\text{false, true}\}$ such that $\perp$ is decreasing, i.e., for any $\mathscr{A}, \mathscr{B} \subseteq \mathscr{P}(E)$

$$\mathscr{A} \subseteq \mathscr{B} \Rightarrow \perp(\mathscr{B}) \Rightarrow \perp(\mathscr{A}). \tag{10}$$

Any $\mathscr{A} \subseteq \mathscr{P}(E)$ for which $\perp(\mathscr{A})$ is true is said to be *overlapping*, otherwise $\mathscr{A}$ is non-overlapping.

Definition 8. A hyperconnectivity class $\mathscr{H} \subseteq \mathscr{P}(E)$ is a set of sets with the following three properties:

(1) $\emptyset \in \mathscr{H}$
(2) $\{x\} \in \mathscr{H}$
(3) for each family $\{C_i\} \subset \mathscr{H}$, $\perp(\{C_i\})$ implies $\cup C_i \in \mathscr{H}$.

As before, both the empty set and singleton sets are hyperconnected, but now any union of hyperconnected sets which are overlapping in the sense of $\perp$ is hyperconnected. In [17] several examples are given to use this

framework for dealing with overlap. However, hyperconnectivities are not shown to be able to deal with the over-partitioning problem of Proposition 1.

5. Attribute spaces and attribute-space filters

As was seen above, connectivities based on partitioning operators yield rather poor results in the attribute filter case. To avoid this, I propose to transform the binary image $X \subset E$ into a higher dimensional *attribute space* $E \times A$ in which A is some space encoding the local properties or attributes of pixels in any image. Scale spaces are an examples of attribute spaces, but other attribute spaces will be explored here. To embed the image in $E \times A$ we use an operator $\Omega : \mathscr{P}(E) \rightarrow \mathscr{P}(E \times A)$, which means $\Omega(X)$ is a binary image in $E \times A$. Typically $A \subseteq \mathbb{R}$ or $\mathbb{Z}$, although the theory presented here extends to cases such as $A \subseteq \mathbb{R}^n$. The inverse operator $\Omega^{-1} : \mathscr{P}(E \times A) \rightarrow \mathscr{P}(E)$, projects $\Omega(X)$ back onto X, i.e., $\Omega^{-1}(\Omega(X)) = X$ for all $X \in \mathscr{P}(E)$. Furthermore, Ω^{-1} must be increasing: $Y_1 \subseteq Y_2 \Rightarrow \Omega^{-1}(Y_1) \subseteq \Omega^{-1}(Y_2)$ for all $Y_1, Y_2 \in \mathscr{P}(E \times A)$. Summarizing we have:

Definition 9. An attribute-space transform pair (Ω, Ω^{-1}) from $E \leftrightarrow E \times A$, is a pair of operators such that:

(1) $\Omega : \mathscr{P}(E) \rightarrow \mathscr{P}(E \times A)$ is a mapping such that for any $X \in \mathscr{P}(E)$, each point $x \in X$ has *at least* one corresponding point $(x, a) \in \Omega(X)$, with $a \in A$,
(2) $\Omega(\emptyset) = \emptyset$,
(3) $\Omega(\{x\}) \in \mathscr{C}_{E \times A}$ for all $x \in E$,
(4) $\Omega^{-1} : \mathscr{P}(E \times A) \rightarrow \mathscr{P}(E)$ is a mapping such that for any $Y \in \mathscr{P}(E \times A)$, every $(x, a) \in Y$ is projected to $x \in \Omega^{-1}(Y)$,
(5) $\Omega^{-1}(\Omega(X)) = X$ for all $X \in \mathscr{P}(E)$,
(6) Ω^{-1} is increasing.

Note that $\mathscr{C}_{E \times A}$ is the connectivity class used in $E \times A$. Furthermore, even though $\Omega^{-1}(\Omega(X)) = X$ for all $X \in \mathscr{P}(E)$, $\Omega(\Omega^{-1}(Y)) = Y$ will not in general hold for all $Y \in \mathscr{P}(E \times A)$. It is trivial to construct a connected set $Y \subseteq E \times A$ such that its projection $\Omega^{-1}(Y)$ onto E is equal Fig. 5(d). However, mapping this back into $E \times A$ using Ω used in Fig. 5 yields a disconnected set in $E \times A$, as shown in Fig. 5(f). Therefore, $\Omega(\Omega^{-1}(Y)) \neq Y$ in this case.

Using the above we can define the notion of *attribute-space connectivity class*.

Definition 10. An attribute-space connectivity class $\mathscr{A} \subseteq \mathscr{P}(E)$ on universal set E generated by an attribute-space transform pair (Ω, Ω^{-1}) and connectivity class $\mathscr{C}E \times A$ on $E \times A$, is defined as

$$\mathscr{A} = \{C \in \mathscr{P}(E) | \Omega(C) \in \mathscr{C}_{E \times A}\} \tag{11}$$

Note that properties 2 and 3 in Definition 9 mean that singletons and the empty set are members of $\mathscr{A}$, as in the case of (hyper)connectivities. Attribute-space connected filters can now be defined as follows.

Definition 11. An attribute-space connected filter $\Psi^A : \mathscr{P}(E) \rightarrow \mathscr{P}(E)$ is defined as

$$\Psi^A(X) = \Omega^{-1}(\Psi(\Omega(X))) \tag{12}$$

with $X \in \mathscr{P}(E)$ and $\Psi : \mathscr{P}(E \times A) \rightarrow \mathscr{P}(E \times A)$ a connected filter, and (Ω, Ω^{-1}) an attribute-space transform pair.

Thus attribute-space connected filters work by first mapping the image to a higher dimensional space, applying a connected filter and projecting the result back. Note that the connected filter Ψ may use second-generation connectivity rather the underlying connectivity in $E \times A$ (e.g., 26-connectivity in 3D). Note that if Ψ is anti-extensive (or extensive), so is Ψ^A due to the increasingness of Ω^{-1}. However, if Ψ is increasing, this property does not necessarily hold for Ψ^A, as will be shown in Section 5.1 and following and Fig. 7. Similarly, idempotence of Ψ does not imply idempotence of Ψ^A. However, if

$$\Psi(\Omega(X)) = \Omega(\Psi^A(X)) = \Omega(\Omega^{-1}(\Psi(\Omega(X)))), \tag{13}$$

for all $X \in \mathscr{P}(E)$, idempotence of Ψ does imply idempotence of Ψ^A, because Ω maps $\Psi^A(X)$ exactly back onto

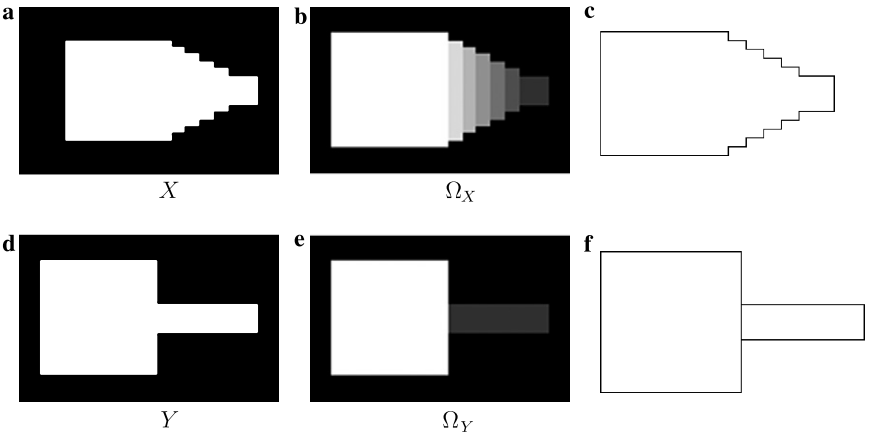

Fig. 5. Attribute-space partitioning of two binary sets: (a) and (d) binary images X and Y each containing a single (classical) connected component; (b) and (e) their respective opening transforms; (c) and (f) partitioning of X and Y using edge strength threshold $r = 1$. X is considered as one component due to the slow change in attribute value, whereas the abrupt change in width causes a split in Y.

$\Psi(\Omega(X))$. Eq. (13) obviously holds when $\Omega(\Omega^{-1}(Y)) = Y$ for all $Y \in \mathscr{P}(E \times A)$, but (13) is slightly more general.

5.1. Width-based attribute spaces

In the following $E = \mathbb{Z}^2$. As an example of mapping of a binary image $X \in \mathscr{P}(E)$ to binary image $Y \in \mathscr{P}(E \times A)$ we can use local width as an attribute to be assigned to each pixel $x \in X$. In this case $A = \mathbb{Z}^+$. We can implement this mapping using an opening transform defined by granulometry $\{\beta_r\}$, in which each operator $\beta_r : E \to E$ is an opening with a structuring elements B_r. An opening transform is defined as

Definition 12. The opening transform Ω_X of a binary image X for a granulometry $\{\beta_r\}$ is

$$\Omega_X(x) = \max\{r \in A | x \in \beta_r(X)\} \tag{14}$$

In the case that $\beta_r(X) = X \circ B_r$ with $\circ$ denoting structural openings and B_r ball-shaped structuring elements of radius r, an opening transform assigns the radius of the largest ball such that $x \in X \circ B_r$. An example is shown in Fig. 5. We can now devise a width-based attribute space by the mapping $\Omega_w : \mathscr{P}(E) \to \mathscr{P}(E \times \mathbb{Z})$ as

$$\Omega_w(X) = \{(x, \Omega_X(x)) | x \in X\} \tag{15}$$

The inverse is simply

$$\Omega_w^{-1}(Y) = \{x \in E | (x, y) \in Y\} \tag{16}$$

with $Y \in \mathscr{P}(E \times \mathbb{Z})$.

Let $\{C_i\} \subset E \times A$ be the set of connected components of $\Omega_w(X)$ with i from some index set. Because a single attribute value is assigned to each pixel by Ω_X, it is obvious that the projections onto E of these sets $C_i^w = \Omega^{-1}w(C_i)$ are disjoint as well. Thus they form a partition of the image plane in much the same way as classical connected components would do, as can be seen in Fig. 5. In this example we can work in a 2D grey-scale image, rather than a 3D binary image, for convenience. Connectivity in the attribute space is now partly encoded in the grey-level differences of adjacent flat zones in these images. In the simplest case, corresponding to 26-connectivity in the 3D binary image, a grey-level difference of 1 means adjacent flat-zones are connected in attribute space. More generally, we can use some threshold r on the grey-level difference between adjacent flat zones. This corresponds to a second-generation connectivity $\mathscr{C}^{\psi_r}$ with ψ_r a dilation in $\mathbb{Z}^3$, with structuring element $\{(0,0,-r),(0,0,-r+1),\ldots,(0,0,r)\}$. The effect of this can be seen in Fig. 5(f), in which abrupt changes in width lead to splitting of a connected component into two parts. Fig. 6 demonstrates that this splitting is different from any caused by a partitioning connectivity. Fig. 7 shows that an attribute-space area operator Ψ^A based on an area opening Ψ in $E \times A$ is not increasing. This effect occurs due to the fact that overlap of X_1 and X_2 in E does not imply overlap of $\Omega_w(X_1)$ and $\Omega_w(X_2)$ in $E \times A$.

A slightly different partitioning is obtained if we change (15) to

$$\Omega_{\log w}(X) = \{(x, 1 + \log(\Omega_X(x))) | x \in X\} \tag{17}$$

with $\Omega_{\log w}^{-1} = \Omega_w^{-1}$. Note that one is added to the logarithm of the width to separate bridges of unity width from the background. Though very similar in behaviour to the attribute-space connectivity using Ω_w, attribute-space connectivity based on $\mathscr{C}^{\psi_r}$ is now scale-invariant, as is shown in Fig. 8. None of the second-generation connectivities in E proposed in [8,9,16] can achieve this, because they are all based on increasing operators based on fixed structuring elements, which are not scale-invariant.

Any nonlinear transformation on the attribute can be used to obtain different results, depending on the application. A simple method is to threshold the opening transform Ω_X assigning foreground pixels to different classes, denoted by Ω_X^t, allowing connectivity only within a class. A simple two-class classification is shown in Fig. 9, in which a second-generation connected attribute filter is compared to the corresponding two-class pixel classification method. Only the attribute-space method distinguishes the normal vessels from the aneurysm properly. Note that this does not represent an optimal, real-world application

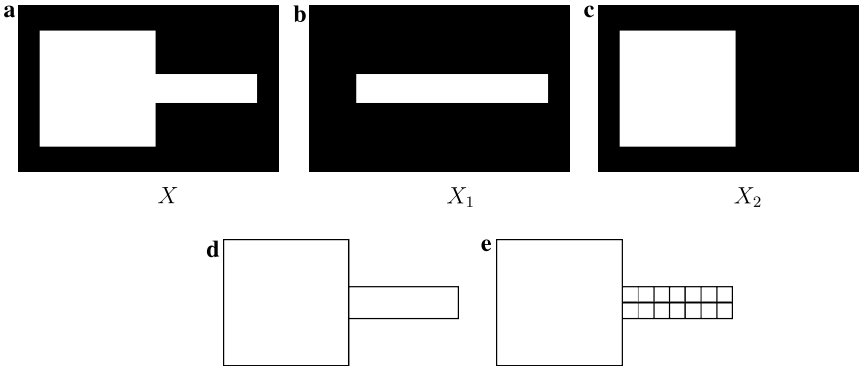

Fig. 6. Attribute-space connectivity is not connectivity: (a) binary image X is the union of two overlapping sets X_1; (b) and X_2; (c) each of which are considered connected in attribute space; however, X is partitioned into two sets; (d) by the same attribute-space connectivity; (e) any partitioning connectivity which separates the square from the elongated part of X splits the elongated part into 14 singletons.

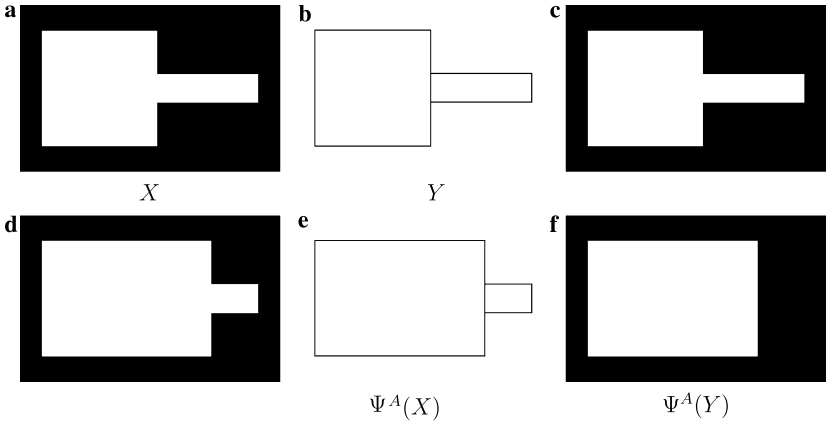

Fig. 7. Ψ^A is not necessarily increasing for increasing Ψ: (a) and (d) binary images X and Y, with $X \subseteq Y$; (b) and (e) partitions of X and Y in attribute space projection of Ω_w; (c) and (f) $\Psi^A(X)$ and $\Psi^A(Y)$, using for Ψ an area opening with area threshold 10. Clearly $\Psi^A(X) \not\subseteq \Psi^A(Y)$, even though Ψ is increasing.

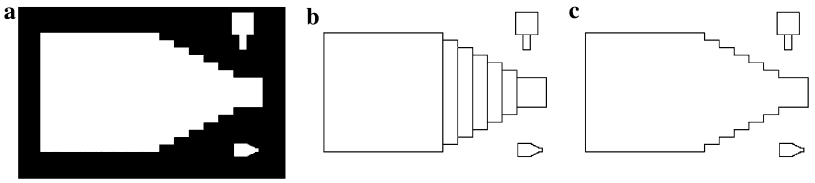

Fig. 8. Scale invariant partitioning using 26-connectivity in 3D: (a) binary image in which the large and the bottom small connected component have identical shapes; (b) partitioning using Ω_w; (c) scale-invariant partitioning using $\Omega_{\log w}$, which splits the top small connected component, but regards the other two as single entities.

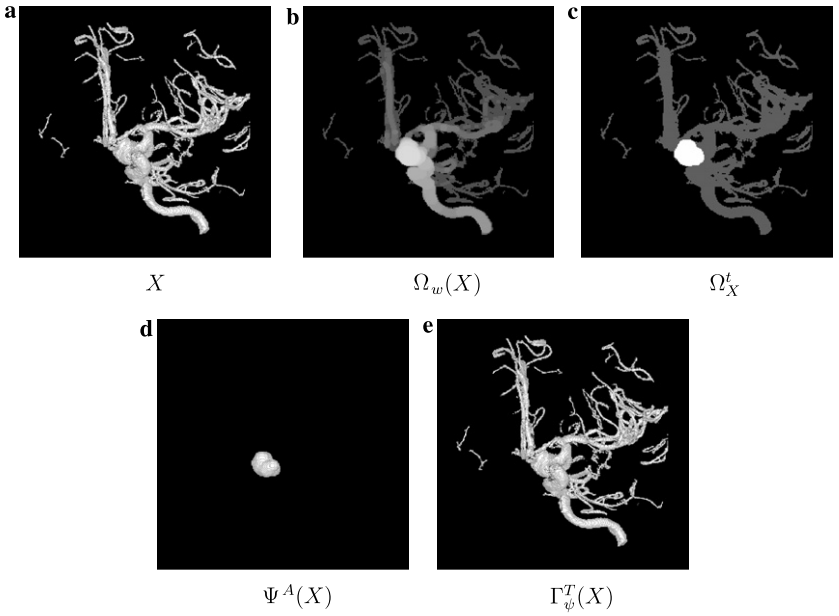

Fig. 9. Elongation filtering and aneurysm detection: (a) ray-cast of a CT angiogram containing an aneurysm; (b) maximum-intensity projection (MIP) of grey-scale representation of width–space transformation $\Omega_w(X)$; (c) same as (b) but for Ω_X^t using $t = 6$; (d) result of elongation filtering *rejecting* features with elongation measure $I/V^{5/3} > 0.5$; (e) Second-generation connected filter result Γ_ψ^T, using same criterium and connectivity based on opening by a B_6, because all voxels in vessels are considered singletons, they are all considered to be compact.

of attribute-space connected attribute filtering, rather, it serves to show what the difference is between the way second-generation connectivity merges the use of anti-extensive, structuring-element-based filters with attribute filtering and the way this is done by attribute-space connectivity. In essence the ''hard work'' of splitting the normal vessels from the aneurysm by the structural opening used, after which the attribute-space connected filter extracts

image features based on the attributes of the "perceptual groups" it obtains.

5.2. Orientation-based attribute spaces

Width is not the only attribute which can be used to subdivide a connected component. In this section orientation is used to create attribute spaces which can deal with overlap as in Fig. 1. Orientation can be measured in a variety of ways [24–26], any of which might be applicable in this framework. Formally, let $A = [0, \pi)$ and $E \times A$ be our attribute space, with toroidal topology in the A dimension (i.e., orientation $\alpha = 0$ is equivalent to $\alpha = \pi$). The operator $\Omega_\alpha : \mathscr{P}(E) \rightarrow \mathscr{P}(E \times A)$ assigns one or more orientation values $\alpha_i \in A$ to every pixel in X. In this case the following method is used:

(1) Compute a series of opening transforms Ω_X^α using linear structuring elements with orientation α.
(2) This yields a grey-level function $f(x, \alpha)$ over the domain $E \times A$.
(3) For each pixel in X, find the minimum value $f_{\min}(x) = \min_{\alpha \in A} f(x, \alpha)$.
(4) For each pixel in X, find the maximum value $f_{\max}(x) = \max_{\alpha \in A} f(x, \alpha)$.
(5) Compute $\Omega_\alpha(X)$ as

$$\Omega_\alpha(X) = \{x \in X, \alpha \in A | f(x, \alpha) > \lambda f_{\min}(x) \vee f(x, \alpha) = f_{\max}(x)\} \tag{18}$$

with $\lambda > 1$ a tunable parameter to select how strict we will be in orientation selectivity.

Two comments must be made: (i) including all points in $X \times A$ for which $f(x, \alpha) = f_{\max}(x)$ ensures all points in X are assigned at least one α-value and (ii) circular objects will show up at any orientation. This orientation space will therefore not separate compact objects with elongated structures attached to them. An example is shown in Fig. 10.

In this case the components of the attribute-space embedding of an image form a *cover* of the image domain rather than a *partition*, as is required for connected filters in Definition 3 [10]. A cover $\{\beta_j\} \subset \mathscr{P}(E)$ is a collection of sets such that

$$\bigcup_j \beta_j = E. \tag{19}$$

The sets β_i and β_j need not be disjoint if $i \neq j$. Therefore, for any pixel x there exists *at least* one j such that $x \in \beta_j$. Restricting ourselves to the connected foreground components, each component $C_j \preccurlyeq \Omega_\alpha(X)$ in attribute space $E \times A$ will result in one element of cover $\{\beta_j\}$ by back projection through Ω_α^{-1}, such that

$$\beta_j = \Omega_\alpha^{-1}(C_j). \tag{20}$$

A pixel x is only removed by attribute operator Ψ^A if all sets β_j such that $x \in \beta_j$ are removed. An example of filtering based on such an attribute space is given in Fig. 11.

This figure also illustrates the that we can define attribute-space granulometries attribute-space shape or size granulometries and spectra in analogy to connected shape or size granulometries [11,18]. A granulometry is defined as a family $\{\alpha_r\}$ of filters with r from some totally ordered set with the following properties:

(1) $\alpha_r(X) \subseteq X$
(2) $X \subseteq Y \Rightarrow \alpha_r(X) \subseteq \alpha_r(Y)$
(3) $\alpha_s(\alpha_r(X)) = \alpha_{\max(r,s)}(X)$

Because the latter condition implies idempotence it is easily seen that all α_r are openings. Let $\{\alpha_r\}$ be a granulom-

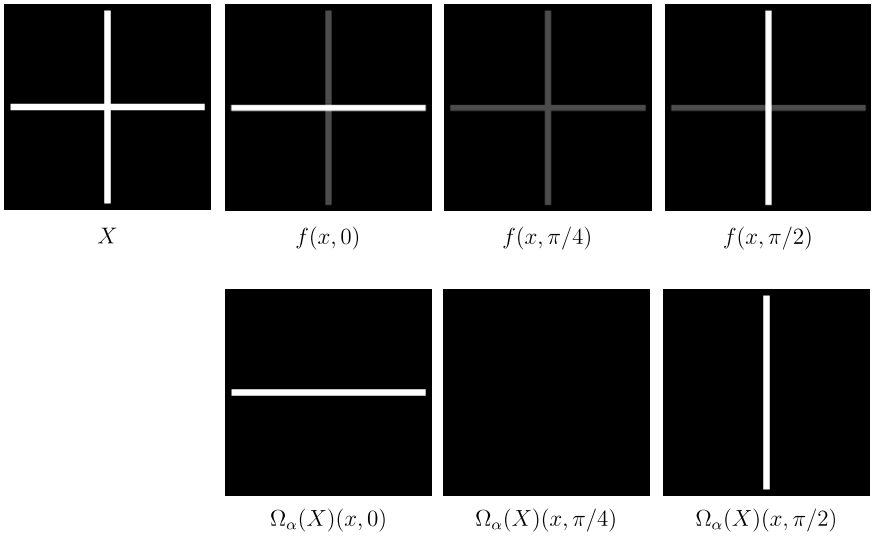

Fig. 10. Orientation-based attribute spaces, a binary image X, the opening transforms $f(x, \alpha) = \Omega_X^\alpha$ with linear structuring elements at orientations $\alpha = 0$, $\alpha = \pi/4$, and $\alpha = \pi/2$, and the slices in attribute space $\Omega_\alpha(X)$ for the same values of α.

Fig. 11. Orientation-based attribute-space connected area granulometry: Parts of the original image are systematically removed by using a sequence of attribute-space area filters, using the same attribute space as in Fig. 10. Filters Γ_λ^A removes all components of $\Omega_\alpha(X)$ the projected area of which is smaller than λ.

etry, with each $\alpha_r : \mathscr{P}(E \times A) \to \mathscr{P}(E \times A)$ a connected filter, with r from some ordered set Λ.

Definition 13. An attribute-space connected granulometry is a set of attribute-space connected filters $\{\alpha_r^A\}$ defined as

$$\alpha_r^A = \Omega^{-1}(\alpha_r(\Omega(X))), \tag{21}$$

with $\{\alpha_r\}$ a granulometry on $\mathscr{P}(E \times A)$ consisting of connected filters; $\{\alpha_r^A\}$ has the following properties

$$\alpha_r^A(X) \subseteq X, \tag{22}$$

$$s \leqslant r \Rightarrow \alpha_r^A(X) \subseteq \alpha_s^A(X) \tag{23}$$

for all $X \subseteq E$.

Note that the stronger nesting property of granulometries, i.e.

$$\alpha_r^A(\alpha_s^A(X)) = \alpha_{\max(r,s)}^A(X) \tag{24}$$

only holds if the condition on idempotence in (13) is true for all α_r in the granulometry. However, property (23) does lead to a nesting of the resulting images $\alpha_r^A(X)$ as a function of r, so pattern spectra f_X^A based on these filters can be defined as

$$f_X^A(r) = \begin{cases} \mu(X \setminus \alpha_r^A(X)) & \text{if } r = 1 \\ \mu(\alpha_{r-1}(X) \setminus \alpha_r^A(X)) & \text{if } r > 1 \end{cases} \tag{25}$$

with μ the Lebesgue measure in E (area in 2D), and $\Lambda = 1, 2, \ldots, N$, similar to [27]. We can safely use the Lebesgue measure in real images, because they are always measurable. Finally, note that connected filters form a special case of attribute-space connected filters, in which $\Omega = \Omega^{-1} = I$, with I the identity operator. Fig. 11 shows how features are removed by an attribute-space granulometry based on area. As the area threshold is increased, larger structures are removed.

Note that the fact that this attribute-space connectivity supports overlap does not by itself mean that it is a hyperconnectivity. For this the third property in Definition 8 must be satisfied. Before this can be done, we need to investigate whether it is possible to formulate an overlap criterion $\perp$ in the sense of Definition 7. One way is which to do this is to use Definition 10, to formulate the following "overlap criterion." Let $\{C_i\} \subseteq \mathscr{A}_\alpha$, with $\mathscr{A}_\alpha$ the attribute-space connectivity class associated with $(\Omega_\alpha, \Omega_\alpha^{-1})$ and $\mathscr{C}_{E\times A}$ defining regular 6-connectivity in $E \times A$. An overlap criterion $\perp_\alpha$ which generates $\mathscr{A}_\alpha$ is

$$\perp_\alpha(\{C_i\}) = \begin{cases} \text{true} & \text{if } \Omega_\alpha(\bigcup_i C_i) \in \mathscr{C}_{E\times A} \\ \text{false} & \text{otherwise.} \end{cases} \tag{26}$$

However, consider the case of a set $\{C_i\}$ of n approximations of line segments of length $2r$ centred on the origin in $\mathbb{Z}^2$, at discrete angles $i\pi/n$ for $i = 0, 1, \ldots, n-1$. For n sufficiently large, the union is equal to a disc of radius r. Therefore

$$\Omega_\alpha(\bigcup_i C_i) \in \mathscr{C}_{E\times A} \Rightarrow \perp_\alpha(\{C_i\}) = \text{true}. \tag{27}$$

However, we have already seen that for $\{C_0, C_{n/2}\}$

$$\Omega_\alpha(C_0 \cup C_{n/2}) \notin \mathscr{C}_{E\times A} \Rightarrow \perp_\alpha(\{C_0, C_{n/2}\}) = \text{false}. \tag{28}$$

Clearly, $\{C_0, C_{n/2}\} \subseteq \{C_i\}$, but $\perp_\alpha(\{C_i\}) \not\Rightarrow \perp_\alpha(\{C_0, C_{n/2}\})$. This violates property (10) in Definition 7.

There may of course be some other overlap criterion which does yield a hyperconnectivity equivalent to $\mathscr{A}_\alpha$, but in general hyperconnectivities and attribute-space connectivities appear to be different.

6. Discussion

Two features determine the success or failure of attribute filters in image processing tasks: (i) determination of suitable properties (attributes) to determine whether a particular image feature is to be rejected or retained and (ii) the grouping method to determine what constitutes an image feature. Attribute-space morphology focusses on the latter part, and solves the problems with attribute filters using partitioning connectivities as noted in Proposition 1. The fragmentation caused by splitting parts of connected components into singletons is absent. This means that attribute-space attribute filters are more than just applying a standard attribute filter to a preprocessed image. The price we pay for this is loss of the increasingness property, and increased computational complexity. In return we may achieve scale invariance, combined with a more intuitive response to, e.g., elongation-based attribute filters, as is seen in Figs. 2 and 9. Note that the over-partitioning problem can also be solved within the framework of connectivity, by using second-generation connectivity based on

maps, or marker images, rather an operator, and changing the second case in (4) [28].

The attribute-space connectivities Ω_w and $\Omega_{\log w}$ from Section 5.1 have a scale parameter, or rather a *scale-difference* or *scale-ratio* parameter. Increasing r in the attribute-space connectivities generated by Ω_w or $\Omega_{\log w}$ combined with $\mathscr{C}^{\psi_r}$ yields a hierarchy, in which the partitioning of $E \times A$ becomes coarser as r is increased. This means we could develop multi-scale attribute-space connectivity or perhaps more properly *multi-level* attribute-space in analogy to the well-defined multi-scale connectivities [15,16] in the future.

In the examples given here A was one-dimensional. In theory it is possible to use multiple dimensions, to represent, e.g., width and orientation. Each dimension could be thought of as analogous to the different sets of neurons in the visual cortex which process different orientations, and different scales [29].

An important feature of this framework is its ability to deal with overlap. No connectivity does this, and the key difference is that attribute-space connected filters rely on *covers* of the image domain rather than *partitions*. It may be possible to develop an even more general framework based on covers, rather than partitions. Future research will focus on grey-scale generalizations and efficient algorithms for these operators. Finally, the relationship to other extensions of connectivity, such as hyperconnectivities and hypoconnectivities [9] needs to be studied further. However, given the fact that set union in the image domain can causes large shifts of subsets of the image X in the attribute space embedding $\Omega(X)$, I do not think it is likely that attribute-space connectivity and hyperconnectivity are the same. There is of course a trivial case of overlap: regular connectivities are special cases of both hyperconnectivities [9] and attribute-space connectivities. Whether any other attribute-space connectivities coincide with hyperconnectivities remains an open question.

References

[1] M. Wertheimer, Principles of perceptual organization, in: D. Beardslee, M. Wertheimer, D. Van Nostrand (Eds.), Readings in Perception, Princeton, NJ, 1958, pp. 115–135.

[2] L.D. Cohen, Multiple contour finding and perceptual grouping using minimal paths, J. Math. Imaging Vis. 14 (2001) 225–236.

[3] Y. Gdalyahu, D. Weinshall, M. Werman, Self-organization in vision: stochastic clustering for image segmentation, perceptual grouping, and image database organization, IEEE Trans. Pattern Anal. Mach. Intell. 23 (2001) 1053–1074.

[4] A. Selinger, R.C. Nelson, A perceptual grouping hierarchy for appearance-based 3D object recognition, Comp. Vis. Image Understand. 76 (1999) 83–92.

[5] P. Kruizinga, N. Petkov, Nonlinear operator for oriented texture, IEEE Trans. Image Process. 8 (1999) 1395–1407.

[6] C. Grigorescu, N. Petkov, M.A. Westenberg, Contour detection based on nonclassical receptive field inhibition, IEEE Trans. Image Process. 12 (2003) 729–739.

[7] T.Y. Kong, A. Rosenfeld, Digital topology: introduction and survey, Comp. Vis. Graph. Image Process. 48 (1989) 357–393.

[8] C. Ronse, Set-theoretical algebraic approaches to connectivity in continuous or digital spaces, J. Math. Imaging Vis. 8 (1998) 41–58.

[9] J. Serra, Connectivity on complete lattices, J. Math. Imaging Vis. 9 (3) (1998) 231–251.

[10] P. Salembier, J. Serra, Flat zones filtering, connected operators, and filters by reconstruction, IEEE Trans. Image Process. 4 (1995) 1153–1160.

[11] E.J. Breen, R. Jones, Attribute openings, thinnings and granulometries, Comp. Vis. Image Understand. 64 (3) (1996) 377–389.

[12] P. Salembier, A. Oliveras, L. Garrido, Anti-extensive connected operators for image and sequence processing, IEEE Trans. Image Process. 7 (1998) 555–570.

[13] P. Monasse, F. Guichard, Fast computation of a contrast invariant image representation, IEEE Trans. Image Process. 9 (2000) 860–872.

[14] H.J.A.M. Heijmans, Connected morphological operators for binary images, Comp. Vis. Image Understand. 73 (1999) 99–120.

[15] C.S. Tzafestas, P. Maragos, Shape connectivity: multiscale analysis and application to generalized granulometries, J. Math. Imaging Vis. 17 (2002) 109–129.

[16] U. Braga-Neto, J. Goutsias, A multiscale approach to connectivity, Comp. Vis. Image Understand. 89 (2003) 70–107.

[17] U. Braga-Neto, J. Goutsias, A theoretical tour of connectivity in image processing and analysis, J. Math. Imaging Vis. 19 (2003) 5–31.

[18] E.R. Urbach, M.H.F. Wilkinson, Shape-only granulometries and grey-scale shape filters, in: Proc. Int. Symp. Math. Morphology (ISMM) 2002, 2002, pp. 305–314.

[19] P. Maragos, R.D. Ziff, Threshold decomposition in morphological image analysis, IEEE Trans. Pattern Anal. Mach. Intell. 12 (1990) 498–504.

[20] A. Sofou, C. Tzafestas, P. Maragos, Segmentation of soilsection images using connected operators, in: Proc. Int. Conf. Image Proc. 2001, 2001, pp. 1087–1090.

[21] G.K. Ouzounis, M.H.F. Wilkinson, Second-order connected attribute filters using Max-trees, in: Mathematical Morphology: 40 Years On, Proc. Int. Symp. Math. Morphology (ISMM) 2005, Paris, 2005, pp. 65–74.

[22] L. Vincent, Morphological area openings and closings for grey-scale images, in: Y.-L.O.A. Toet, D. Foster, H.J.A.M. Heijmans, P. Meer (Eds.), Shape in Picture: Mathematical Description of Shape in Grey-level Images, NATO, 1993, pp. 197–208.

[23] A. Meijster, M.H.F. Wilkinson, A comparison of algorithms for connected set openings and closings, IEEE Trans. Pattern Anal. Mach. Intell. 24 (4) (2002) 484–494.

[24] P. Soille, H. Talbot, Directional morphological filtering, IEEE Trans. Pattern Anal. Mach. Intell. 23 (2001) 1313–1329.

[25] F. le Pouliquen, C. Germain, P. Baylou, Scale-adaptive orientation estimation, in: Proc. 16th Int. Conf. Pattern Rec., Vol. 1, Québec City, Canada, 2002, pp. 688–691.

[26] B. Rieger, L.J. van Vliet, Representing orientation in n-dimensional spaces, in: N. Petkov, M.A. Westenberg (Eds.), Proc. Comput. Anal. Images Patterns 2003, Vol. 2756 of Lecture Notes in Computer Science, Groningen, The Netherlands, 2003, pp. 17–24.

[27] P. Maragos, Pattern spectrum and multiscale shape representation, IEEE Trans. Pattern Anal. Mach. Intell. 11 (1989) 701–715.

[28] G.K. Ouzounis, M.H.F. Wilkinson, Countering oversegmentation in partitioning-based connectivities, in: Proc. Int. Conf. Image Proc. 2005, Genova, Italy, 2005, pp. 844–847.

[29] D.H. Hubel, T.N. Wiesel, Receptive fields and functional architecture of monkey striate cortex, J. Physiol. 195 (1968) 215–243.